International Journal of Solids and Structures 48 (2011) 144–152

Contents lists available at ScienceDirect

International Journal of Solids and Structures

journal homepage: www.elsevier.com/locate/ijsolstr

Modelling creep tests in HMPE fibres used in ultra-deep-sea mooring ropes

H.S. da Costa Mattos [a,*], F.E.G. Chimisso [b]

[a] PGMEC – Laboratório de Mecânica Teórica e Aplicada, Universidade Federal Fluminense, 24210-240 Niterói, RJ, Brazil
[b] POLICAB – Laboratório de Análise de Tensões, Escola de Engenharia, Fundação Universidade Federal do Rio Grande, 96201-900 Rio Grande, RG, Brazil

ARTICLE INFO

Article history:
Received 25 November 2009
Received in revised form 15 August 2010
Available online 25 September 2010

Keywords:
HMPE mooring ropes
Continuum damage mechanics
Creep
Lifetime prediction
Viscoelasticity

ABSTRACT

Due to its low density and high strength, HMPE (high modulus polyethylene) fibres are being increasingly used in synthetic ropes for offshore mooring. Nevertheless, the occurrence of creep at sea temperature can be a shortcoming for its practical use. Creep tests performed at different load levels in a sub-system of the HMPE rope (yarn) are frequently used as a first step to obtain some information about the susceptibility to creep deformation at a given temperature. The present paper is concerned with the phenomenological modelling of creep tests in HMPE yarns. In this macroscopic approach, besides the classical variables (stress, total strain), an additional scalar variable related with the damage induced by creep process is introduced. An evolution law is proposed for this damage variable. The predicted lifetimes and elongations of HMPE specimens in creep tests at different load levels and room temperature are compared with experimental results showing a good agreement.

1. Introduction

Offshore oil drilling and exploration in increasingly deep waters requires the replacement of traditional steel wire rope and chain moorings by synthetic fibre ropes with lesser linear weight. A mooring system with synthetic fibre ropes can be configured as either a catenary or a "taut-leg" system, but generally the last one is the most feasible in deep and ultra-deep waters (Fig. 1, also see the recommended practice for design, manufacture, installation, and maintenance of synthetic fibre ropes for offshore mooring, API-RP, 2001, for instance). Nowadays these synthetic ropes provide the necessary compliance to the taut-leg system by means of the natural mechanical properties of the fibres.

Most fibre ropes comprise a core to withstand tensile loads and an outer jacket, which often has little tensile load bearing capability. Additional protective coatings or wrappings may be applied after rope manufacture. Typical rope construction types suitable for deepwater fibre moorings are wire rope constructions (WRC), and parallel strand types. The main structural levels in a fibre rope, although not all present in every construction, are: (i) textile yarns, as made by the fibre producer and typically consisting of hundreds of individual filaments; (ii) rope yarns, assembled from a number of textile yarns by the rope maker; (iii) strands made up from many rope yarns; (iii) sub-ropes of several strands; (v) the complete core rope assembly; (v) rope, sub-rope and strand jackets.

In the "taut-leg" mooring system, each rope is stretched under tensile load (Fig. 1). Polymer based fibre ropes generally have a rate-dependent nonlinear behaviour. High tenacity Polyester and High Modules Polyethylene (HMPE) are the most common types of synthetic fibres materials used for such kind of offshore mooring ropes. Polyester fibres do not present significant creep at loads and temperatures normally experienced in mooring applications. HMPE is a material with better tensile strength and lower density than polyester, but may present creep even at sea water temperature (Smeets et al., 2001; Chimisso, 2009, for instance). The stability control of the platforms and reliability of the overall mooring system in long term experience with HMPE is a major concern.

It is not the goal of the present paper to goal to discuss the chemical aspects of high modulus polymers neither to investigate the microscopic mechanisms of creep in this kind of material. Such a discussion can be found in other works concerned about the subject. For a general idea of previous studies about this subjects it is suggested the works of Ward and colleagues (Ciferri and Ward, 1979; Ward and Sweeney, 2004; Wilding and Ward, 1981, 1984a,b; Bonner et al., 1999, for instance) and also the papers of Liu et al. (2008) and Kolarik et al. (2006).

Many studies particularly concerned with polymer fibres, ropes and fabrics have also been developed in the last years (Boxman and Cloos, 1998; Smeets et al., 2001; Bles et al., 2009; Ghoreishi et al., 2007; Fernandes and Rossi, 2005; King et al., 2005, for instance). Nevertheless, the mechanisms proposed so far to explain the damage initiation and propagation processes in different geometry/material mooring systems are not able to elucidate all aspects of the phenomenon (Pellegrin, 1999; Sloan, 1999; Hooker, 2000;

* Corresponding author. Tel./fax: +55 21 2629 5585.
E-mail address: heraldo@mec.uff.br (H.S. da Costa Mattos).

0020-7683/$ - see front matter © 2010 Elsevier Ltd. All rights reserved.
doi:10.1016/j.ijsolstr.2010.09.015

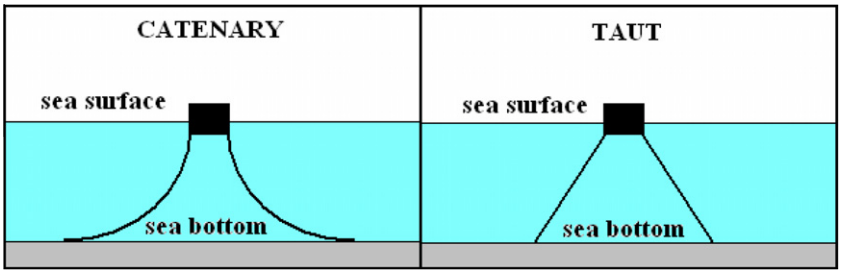

Fig. 1. Catenary and taut leg mooring systems.

Pearson, 2002; Petruska et al., 2005; Silva and Chimisso, 2005; Beltran and Williamson, 2005; Schmidt et al., 2006, for instance).

The study of creep damage and rupture in HMPE ropes is a basic requirement for safe and economic operation for deep water mooring of FSOP units and floating platforms. Nevertheless, the analysis of creep phenomenon accounting for different rope constructions can be extremely complex. Creep tests performed at different load levels in a sub-system of the HMPE rope (yarn) are frequently used as a first step to obtain some information about the susceptibility to creep deformation at a given temperature. However, it is necessary a large number of tests in order to provide basic parameters to be directly used in engineering design, mainly to estimate the influence of the load and temperature on the creep process. Hence, attempts to model these tests are advisable, since a reasonably accurate modelling would require a smaller number of experiments (only the necessary to identify the material parameters that arise in the theory), avoiding the waste of time and consequently reducing costs.

The present paper is concerned with the phenomenological modelling of creep tests of HMPE yarns at room temperature. Yarn is a generic term for a bundle of untwisted or twisted fibres. In the present paper the term yarn is used for the untwisted bundle as provided by the fibre producer and typically consisting of hundreds of individual filaments. The goal is to propose a one-dimensional phenomenological viscoelastic model that combines enough mathematical simplicity to allow its usage in engineering problems with the capability of describing a complex non-linear mechanical behaviour.

The basic idea of a simplified phenomenological modelling of creep tests in HMPE yards is to approximate the specimen subjected to a constant load through a nonlinear viscoelastic "spring". Both systems (real specimen and "equivalent" nonlinear spring) have the same elongation δ at any time instant t when submitted to a constant load F_o (see Fig. 2). The approach is similar to the studies performed in Sampaio et al. (2004) and Costa-Mattos et al. (2008) and the model equations are developed within a thermodynamic framework summarized at the Appendix. In order to account for the dissipative mechanism of rupture, a macroscopic auxiliary damage variable $D \in [0,1]$, related to the loss of the global stiffness of the yarn due to the damage (rupture of some of the fibres, etc.), is introduced. If $D = 0$, the system is undamaged and if $D = 1$, it is "broken" (it can no longer resist to mechanical loading). The modelling of the "equivalent" spring is then reduced to define an adequate expression for the evolution of the damage variable D.

Results from experimental creep tests of Dyneema® SK75 HMPE multi-filaments under different loading are compared with model prediction showing a good correlation.

2. Material and experimental procedures

In this paper it is considered the smallest yarn-like component of the rope, as received from the yarn producer. Such a basic yarn is nothing else than a bundle of untwisted fibres of Dyneema® SK75. All tests were performed in these multi-filaments. This HMPE fibre is produced from the ultra high molecular weight polyethylene (UHMW-PE) by the gelspinning process. In this process the molecules of UHMW-PE fibre are dissolved in a solvent. The obtained solution is successively pulled through small holes and afterwards solidified by cooling it. This process produces a fibre with a chemical structure composed by chains with a high molecular orientation degree (over 95%). This molecular structure, with high crystalline degree (up to 85%) and a little amorphous content, gives the fibre a high modulus and a high rupture load.

The stress σ at a given instant t can be defined as the rate between the applied tensile force $F(t)$ and the average yarn fibre area A_o

$$\sigma(t) = \frac{F(t)}{A_o}; \quad A_o = \frac{\rho_l}{\rho} \Rightarrow \sigma(t) = F(t)\left(\frac{\rho}{\rho_l}\right) \tag{1}$$

where ρ_l is the mass of fibre per unit length and ρ the mass density of fibre material. Since the mass density ρ is the same for a given polymer material, to define the stress of a general yarn regardless the number of fibres it is only necessary to consider the tensile force F divided by the mass of fibre per unit length ρ_l:

$$\hat{\sigma}(t) = \frac{\sigma(t)}{\rho} = \frac{F}{\rho_l} \tag{2}$$

Dyneema® SK75 HMPE multi-filaments considered in this work have linear weight $\rho_l = 1760$ dtex (where 1 dtex = 1 g/10,000 m). dtex is the most used unit for linear density of a yarn in textile industry and hence it will be adopted on the present study. Each specimen with initial length $L_o = 500 \pm 1$ mm was initially loaded at a rate $\alpha = 8.3$ N/s until a limit constant load F_o. Fig. 3 shows the typical loading history the specimens are submitted to.

The strain ε at a given instant t can be defined as the rate between the elongation $\delta(t)$ and the initial length L_o

$$\varepsilon(t) = \frac{\delta(t)}{L_o} \tag{3}$$

2.1. Creep and tensile tests in HMPE yarns

The experimental tests on synthetic fibres used to made ropes in general or specific offshore mooring ropes, developed inside scientific or rope maker laboratories, follow specific standards (API, ISO, ASTM, Cordage Institute). In these standards, rules and recommendations are established regarding sample, dimensions of the specimens, range of speed for the test machine, types of clamps, ideal condition of temperature and humidity and so on.

Usually, the tensile tests are realized to determine mechanical characteristics like yarn break load (YBL), final elongation and tenacity for the mono or multi-filaments that compose a yarn. For most types of synthetic fibres, thee mechanical characteristics, are identified in servo-hydraulic or in electromechanical test machines using

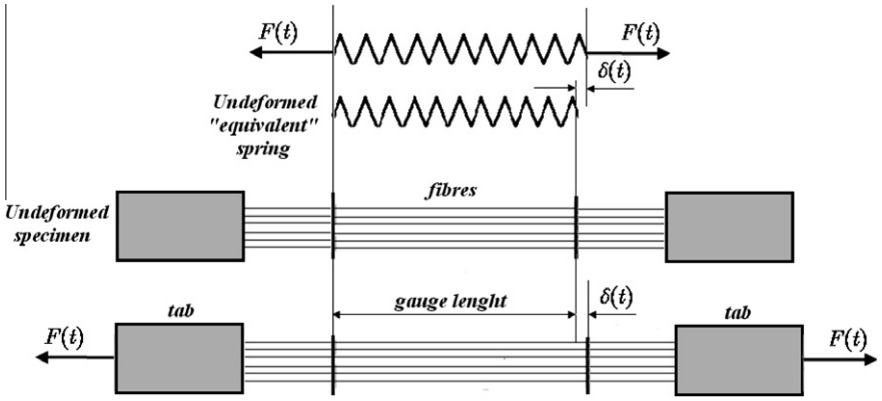

Fig. 2. Creep test specimen and equivalent spring system.

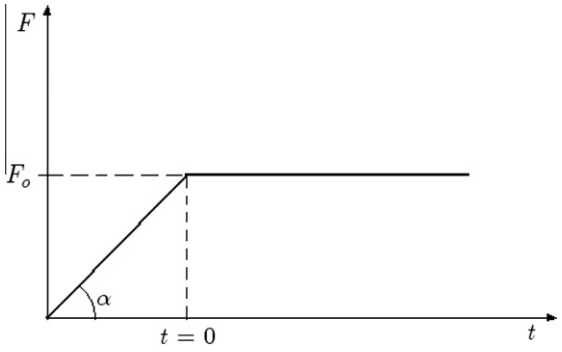

Fig. 3. Typical loading history in a creep test.

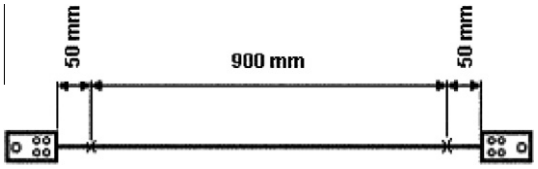

Fig. 4. Long-term creep test – specimen dimensions.

spool clamps or pneumatic clamps. Each head of the testing machine shall carry one grip for holding the test specimen so that the direction of the force applied to the specimen is coincident with the longitudinal axis of the specimen. The grips shall apply sufficient lateral pressure to prevent slippage between the grips face and the fibres. Eventually a tab (a plate made of fibre-reinforced plastic, aluminium or other material) is bonded to the test specimen to transmit loads from the testing machine to the test portion.

Classical tensile and creep tests realized in samples of synthetic fibres used to make ropes, like Nylon, Polyester, Polypropylene, and Polyethylene, follow the above mentioned rules and do not demand the use of tabs at the extremities. Nevertheless, the very low friction coefficient of HMPE filaments makes very difficult to perform these tests without the tabs at the extremities of the specimen to avoid slippage between fibres and clamps. To overcome this problem, the specimens had specially developed tabs at their ends (Fig. 4).

2.1.1. Tensile rupture test

Tensile tests were performed in an electromechanical test machine with special pneumatic clamps for yarn tests, with a 1 kN capability load cell. All tests were performed using a constant rate of $\alpha = 8.3$ N/s in an atmosphere controlled room, with the following conditions: 55 ± 2% of humidity and 20 ± 2 °C temperature. The specimens had initial gauge length of 500 ± 1 mm and the average yarn breaking load (YBL) after 10 tests was 573.3 N. Hence the average rupture stress $\bar{\sigma}_r$ for any multi-filament of this particular HMPE is given by $(F_r/\rho_l) = 575.3/1760 \approx 0.33$ N/dtex.

2.1.2. Long term creep tests

The tests there were performed using constant loads of 15% and 30% of the average YBL (5 test per load levels). Such values are reasonably representative of the tensile loading a synthetic mooring line in a taut-leg configuration can face in operation. For a storm condition, the maximum solicitation of a mooring line should not exceed 30% of MBL (Minimum Break Load) of the rope. For normal work conditions, the rope solicitation should be at least 15% of the MBL of the rope. All tests with loads smaller than 30% of the average YBL will be called in this paper *long term creep tests* since the time necessary rupture of the specimen is superior to one year (eventually there is no creep damage for very low load levels).

These long term creep tests were performed using a "dead weight" device. The length of the specimens used in these tests was 1000 mm, and the gauge length L_o is 900 ± 1 mm, 50 mm adjacent to each termination, as shown in Fig. 4.

In each specimen the ends of the multifilament were glued with an epoxy resin between two wooden plates and mounted in aluminium supports pressed by screws, like a sandwich, as shown in Fig. 5.

2.1.3. Creep rupture tests

All tests performed with load levels higher than 30% of the average YBL until rupture will be called in this paper *Creep rupture tests*. Although these load levels are higher than the ones a yarn can face in operation, they must be considered to obtain creep failure in a short period of time. As it is shown in the next section, the time to failure at a given load level (at least two different load levels) is essential in order o identify the material parameters that appear in the evolution law proposed for the damage variable.

In these creep rupture tests a similar sandwich termination was used (without the steel plates). The specimens were fixed to the machine clamps like a sandwich formed by multifilament glued with an epoxy resin inside two polyvinyl sheets. It was been applied testing loads corresponding approximately to 60%, 70%, 75%, 80%, 85%, and 90% of the mean YBL. An initial gauge length of 500 ± 1 mm was adopted, considering an equal distance between the ends of the specimen after applying a pretension of 1 N (ASTM D885 (1998)).

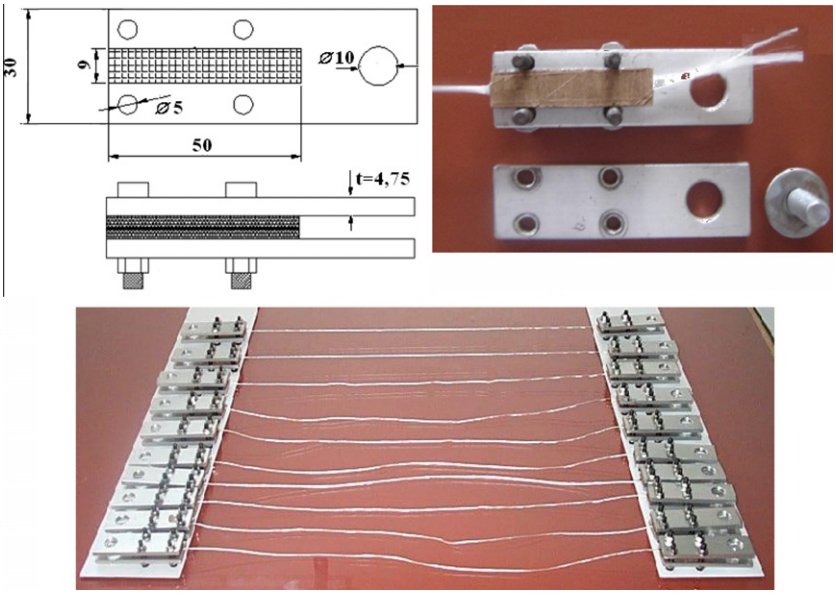

Fig. 5. Long-term creep test specimens.

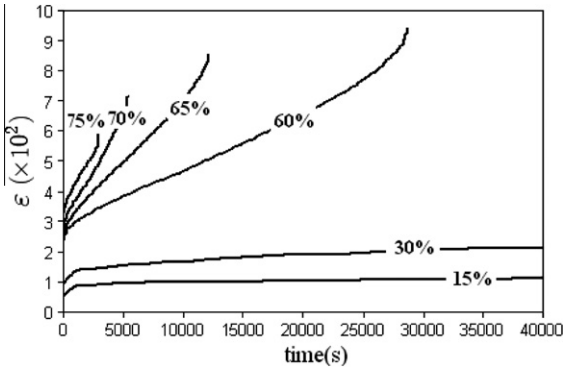

Fig. 6. Experimental creep curves at different load levels.

3. Results and discussion

3.1. Creep testing – elongation curves at different load levels

Fig. 6 shows experimental creep curves at different load levels (level 1: F_o = 86.3 N; level 2: F_o = 172.6 N; level 3: F_o = 345.3 N; level 4: F_o = 374.0 N; level 5: F_o = 402.7 N; level 6: F_o = 431.5 N). The rupture force in a tensile test with prescribed load history $F(t) = \alpha t$ is dependent of the rate α. For the rate α = 8.3 N/s, the average YBL obtained in the tensile tests is 573.3 N.

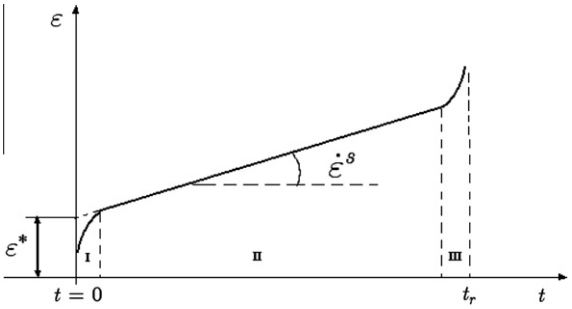

Fig. 7. Typical creep curve.

Table 1
Experimental creep lifetimes for different load levels.

F_o (N)	t_r (s)
345.3	28,710
374.0	12,162
402.7	5425
431.5	2935

From Fig. 6 it is possible to observe that a typical experimental curve shows three stages (see Fig. 7): (i) a "primary creep" phase during which hardening of the material leads to a decrease in the rate of flow which is initially very high; (ii) a "secondary" creep phase during which the rate of flow is almost constant; (iii) a "tertiary" creep phase during which the strain rate increases up to fracture.

It can be verified that the load level strongly affects the creep deformation rate and creep lifetime. Table 1 presents the experimental lifetimes obtained for different load levels. The secondary creep rates $\dot{\varepsilon}^s$ for different load levels are depicted in Table 2.

The strain ε^* (see graphical definition in Fig. 7) for different load levels is presented in Table 3. ε^* is related to the secondary creep and depends on the loading rate α and of the maximum force level F_o.

Average of 5 tests for each load level were taken for the determination of lifetime, secondary creep rate $\dot{\varepsilon}^s$ and strain ε^* of the samples.

3.2. Modelling

In this paper, in order to provide a better understanding of the results from creep tests, a simple one-dimensional model is proposed. The main goal is to present model equations that combine enough mathematical simplicity to allow their usage in engineering problems with the capability of describing a complex non-linear mechanical behaviour. All the proposed equations can be developed from thermodynamic arguments presented at the Appendix. In order to build the model, it is considered as a system a tension specimen with gauge length L and a mass of fibre per unit length ρ_l submitted to a prescribed elongation $\delta(t)$. The following

Table 2
Experimental secondary creep rate for different load levels.

F_o (N)	$\dot{\varepsilon}^s$ (s^{-1})
86.3	14×10^{-9}
172.6	94×10^{-8}
345.3	17×10^{-7}
374.0	39×10^{-7}
402.7	58×10^{-7}
431.5	74×10^{-7}

Table 3
Experimental values of ε^* for different load levels.

F_o (N)	ε^*
86.3	1.02×10^{-2}
172.6	1.73×10^{-2}
345.3	2.79×10^{-2}
374.0	3.05×10^{-2}
402.7	3.18×10^{-2}
431.5	3.37×10^{-2}

model is proposed to describe the creep damage behaviour of HMPE multifilaments:

$$F_o = (1-D)\rho_l E_l(\varepsilon - \varepsilon_v) \tag{4}$$

$$\dot{\varepsilon}_v = \frac{K}{(1-D)}\left[\exp\left(\frac{N_l F_o}{\rho_l}\right) - 1\right];$$
$$\varepsilon_v(t=0) = \varepsilon^* = \frac{F_o}{\rho_l E_l} + \left(\frac{a_l F_o}{\rho_l}\right)^b \tag{5}$$

$$\dot{D} = \left(\frac{S_l F_o}{\rho_l(1-D)}\right)^R; \quad D(t=0) = 0 \tag{6}$$

where ε, ε_v are defined as follows:

$$\varepsilon = (\delta/L); \quad \varepsilon_v = (\delta_v/L); \quad \delta = \delta_e + \delta_v \tag{7}$$

with δ_e being the elastic or reversible part of δ and δ_v the irreversible parcel of δ. $\dot{\varepsilon}_v$ and $\dot{D}$ are, respectively, the material time derivatives of the variables ε_v, D.

The basic idea is to introduce a macroscopic variable $D \in [0,1]$, related to the loss of stiffness of the specimen due to creep damage. If $D = 0$, the specimen is considered "virgin" and if $D = 1$, it can no longer resist to mechanical loading. E_l, K, N_l, S_l , R, a_l, b are positive material constants which depend on the material. Eq. (4) will be called the state law and Eqs. (5) and (6) the evolution laws.

Using boundary condition $D(t = 0) = 0$, it is possible to find the analytical solution of differential Eq. (6) that governs the damage evolution in a constant load (creep) test:

$$D(t) = 1 - \left[1 - \left(t(R+1)\left(\frac{S_l F_o}{\rho_l}\right)^R\right)\right]^{\frac{1}{R+1}} \tag{8}$$

Since rupture occurs when $D = 1$, it is possible to compute the time t_r until the rupture

$$D = 1 - \left(1 - \frac{t}{t_r}\right)^{\frac{1}{(R+1)}} \quad \text{with} \quad t_r = \frac{1}{(R+1)}\left(\frac{S_l F_o}{\rho_l}\right)^{-R} \tag{9}$$

From the equations here proposed it is possible to observe that during the creep test the damage variable increases slowly until almost the end of the test ($t = t_r$) when it increases very fast until rupture ($D = 1$), as it is shown in Fig. 8.

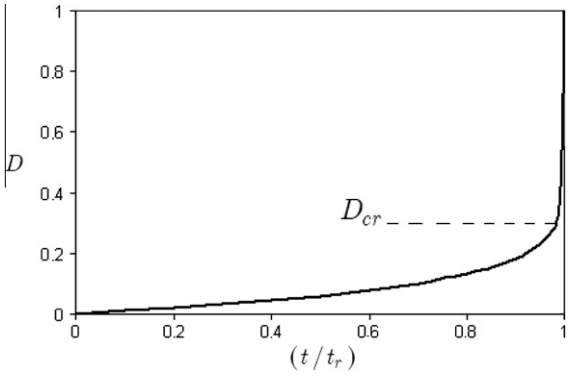

Fig. 8. Damage evolution in a creep test.

If this kind of damage behaviour is observed, it is usual to consider a critical value D_{cr} of the damage variable, beyond which the evolution to the value toward $D = 1$ is so fast that it can be considered instantaneous. If, in a conservative approach, the failure is considered to occur when $D = D_{cr}$, the following expression is obtained

$$D = 1 - \left[1 - \left(\frac{t}{t_{cr} + \frac{(1-D_{cr})^{(R+1)}}{R+1}\left(\frac{S_l F_o}{\rho_l}\right)^{-R}}\right)\right]^{\frac{1}{R+1}} \tag{10}$$

with $t_{cr} = \frac{1-(1-D_{cr})^{(R+1)}}{R+1}\left(\frac{S_l F_o}{\rho_l}\right)^{-R}$

From Eq. (9) or (10), the curves of the damage evolution for creep tests under different conditions may be obtained. Examples of these curves are shown in the next section. As it is shown in the next section, the secondary and tertiary stages of the creep curve are fully described by this model. In this model, important parameters, such as steady state elongation rate, and time to failure are also taken into account.

The variables R and S can be identified experimentally from the lifetimes obtained in two creep tests at different load levels, since the behaviour of the $\log(t_r) \times \log(F_o)$ curve is linear, as shown in Eq. (11)

$$t_r = \frac{1}{R+1}\left(\frac{S_l F_o}{\rho_l}\right)^{-R} = \underbrace{\left(\left(\frac{S_l}{\rho_l}\right)^{-R}\frac{1}{R+1}\right)}_{\alpha}(F_o)^{-R} \Rightarrow \log(t_r)$$
$$= \log(\alpha) - R\log(F_o) \tag{11}$$

Parameters K and N_l can be obtained from the secondary creep rate ($\dot{\varepsilon}^s$). Supposing that damage is negligible at secondary creep ($D \approx 0$) and that $\dot{\varepsilon}_v \approx \dot{\varepsilon} = \dot{\varepsilon}^s$ it is possible to obtain

$$\dot{\varepsilon}^s \approx K\left[\exp\left(\frac{N_l F_o}{\rho_l}\right) - 1\right] \text{ at secondary creep} \tag{12}$$

K and N_l can be identified using a minimum square technique. Nevertheless, for practical purposes, it is suggested to initially consider the law $\dot{\varepsilon}^s = \widehat{K}\exp\left(\frac{\widehat{N}F_o}{\rho_l}\right)$. $\widehat{K}$ and $\widehat{N}$ can be identified experimentally from the secondary creep strain rates obtained in two tests at different load levels, since the behaviour of the $\log(\dot{\varepsilon}^s) \times F_o$ curve is linear, as shown in Eq. (13)

$$\ln(\dot{\varepsilon}^s) = \ln(\widehat{K}) + \left[\frac{\widehat{N}}{\rho_l}\right]F_o \tag{13}$$

K and N_l are very close to $\widehat{K}$ and $\widehat{N}$, and can be approximated (from $\widehat{K}$ and $\widehat{N}$) using the following iterative procedure:

(a) $i = 0$;
(b) $N_l^i = \widehat{N}; K^i = \widehat{K}$;
(c) Compute K^{i+1} from $\ln(\dot{\varepsilon}^s) = \ln(K^{i+1}) + \ln\left[\exp\left(\frac{N_l^i F_o}{\rho_l}\right) - 1\right]$;
(d) Once K^{i+1} is known, compute N_l^{i+1} using

$$\ln(\dot{\varepsilon}^s) = \ln(K^{i+1}) + \ln\left[\exp\left(\frac{N_l^{i+1} F_o}{\rho_l}\right) - 1\right]$$

(e) $i = i + 1$;
(f) If $i < i_{\max}$ go to (c). Else $K = K^{i+1}$ and $N_l = N_l^{i+1}$.
$i_{\max}$ is the maximum allowed number of interactions (suggestion: $i_{\max} = 5$). More sophisticated convergence criteria can be adopted, but they will not be discussed in this paper.

A typical loading history in a creep test is shown at Fig. 3. A fixed rate $\alpha = 8.3$ N/s is used to reach the constant value F_o of the creep test (taken as instant $t = 0$). The initial strain ε^* (see definition in Fig. 7) is dependent of the force F_o. Expression for ε^* in Eq. (5) is a simplified relation that accounts for the nonlinear relation between the initial deformation ε^* and F_o. The strain ε^* at instant $t = 0$ is supposed to be given by the following relation (Eq. (5)):

$$\varepsilon^* = \underbrace{\frac{F_o}{\rho_l E}}_{\text{elasticity}} + \underbrace{\left(\frac{a_l}{\rho_l}\right)^b (F_o)^b}_{\text{primary creep}} \tag{14}$$

The first parcel of ε^* ate the right side of Eq. (14) is the elastic deformation and the second parcel corresponds to the inelastic deformation after primary creep. Parameters a_l and b can be obtained from two creep tests at different load levels, since the behaviour of the $\log(\bar{\varepsilon}^*) \times \log(F_o)$ curve is linear, as shown in Eq. (15)

$$\ln(\bar{\varepsilon}^*) = b\left[\ln\left(\frac{a_l}{\rho_l}\right) + F_o\right]; \quad \bar{\varepsilon}^* = \varepsilon^* - \frac{F_o}{\rho_l E} \tag{15}$$

An explicit analytic expression for the creep deformation can be obtained using (5) and (9). Using these equations it is possible to obtain:

$$\dot{\varepsilon}_v = \frac{K}{(1-D)}\left[\exp\left(\frac{N_l F_o}{\rho_l}\right) - 1\right] \Rightarrow \dot{\varepsilon}_v = \underbrace{K\left[\exp\left(\frac{N_l F_o}{\rho_l}\right) - 1\right]}_{\dot{\varepsilon}^s}$$

$$\left(1 - \frac{t}{t_r}\right)^{-\left[\frac{1}{R+1}\right]} = \dot{\varepsilon}^s \left(1 - \frac{t}{t_r}\right)^{\underbrace{-\left[\frac{1}{R+1}\right]}_{\beta}}$$

with $\varepsilon_v(t = 0) = \varepsilon^*$. Hence

$$\int_{\varepsilon^*}^{\varepsilon_v} d\varepsilon_v = \int_0^t \dot{\varepsilon}^s \left(1 - \frac{t}{t_r}\right)^{-\beta} dt \Rightarrow \varepsilon_v - \varepsilon^* = \left(\frac{\dot{\varepsilon}^s t_r}{1-\beta}\right)\left[1 - \left(1 - \frac{t}{t_r}\right)^{(1-\beta)}\right]$$

$$\Rightarrow \varepsilon_v = \left(\frac{K\left[\exp\left(\frac{N_l F_o}{\rho_l}\right) - 1\right] t_r}{1-\beta}\right)\left[1 - \left(1 - \frac{t}{t_r}\right)^{(1-\beta)}\right] + \varepsilon^*$$

Finally, using (4), the following expression is obtained:

$$\varepsilon = \frac{F_o}{(1-D)\rho_l E_l} + \varepsilon_v \Rightarrow \varepsilon = \frac{F_o}{\rho_l E_l}\left(1 - \frac{t}{t_r}\right)^{-\beta} + \left(\frac{K\left[\exp\left(\frac{N_l F_o}{\rho_l}\right) - 1\right] t_r}{1-\beta}\right) \times \left[1 - \left(1 - \frac{t}{t_r}\right)^{(1-\beta)}\right] + \frac{F_o}{\rho_l E_l} + \left(\frac{a_l F_o}{\rho_l}\right)^b \tag{16}$$

3.3. Comparison with experimental results

In order to investigate the adequacy of the model presented here, samples of HMPE multifilaments were tested and the experimental results were checked with the model. The model parameters identified experimentally at room temperature are presented in Table 4. All material parameters were identified from the creep tests performed at 65% and 70% of the average YBL.

The model prediction of secondary creep rate $\dot{\varepsilon}^s$ (Eq. (12)) for different load levels is presented in Fig. 9 and Table 5.

The predicted values ε^* of the deformation at the beginning of the creep test using Eq. (14) is presented in Fig. 10 and Table 6.

The experimental and predicted creep lifetimes for different load levels using Eq. (9) are presented in Table 7 and Fig. 11.

Finally, Fig. 12 shows the theoretical and experimental creep curves at different load levels. The model prediction of the fracture time and elongation before rupture are in good agreement with the experimental results.

The initial stages of the creep curves are dependent on the loading history (stress and strain rates) adopted to reach the constant load F_o. Nevertheless, the final stages of the elongation-time curves (secondary and tertiary creep) seem to be little affected by this previous loading history.

4. Conclusions

The proposed model equations combine enough mathematical simplicity to allow their usage in engineering problems with the capability to perform a physically realistic description of inelastic deformation, strain hardening, strain-softening, strain-rate sensitivity and damage observed in creep tests performed in HMPE multifilaments at different load levels. The main idea is to use the model to obtain the maximum information about macroscopic properties of HMPE yarns from a minimum set of laboratory tests. Only two creep tests (two load levels) are required to identify the material constants K, N, R and S that appear in the evolution law for the auxiliary variables ε_v and D. In the present study these material parameters were identified from creep tests performed at 65% and 70% of the rupture load. The agreement between theoretical prevision and experiment is good for creep tests performed at different load levels (15%, 30%, 60% and 75% of the rupture load), what indicates a reasonable coherence of the model and motivates the prosecution of the study. Nevertheless, it is important to observe that the present paper is only a first step towards the modelling of creep tests in HMPE ropes using continuum damage mechanics and that the model validation still requires a complete experimental program (adequate to evaluate standard deviations and allowing to perform an statistical analysis).

The analysis of creep behaviour of mooring lines accounting for the different rope constructions can be extremely complex. The mechanisms proposed so far to explain the damage initiation and propagation processes are not able to elucidate all aspects of the phenomenon in different geometry/material systems. However, in normal operation conditions, the tensile load in synthetic mooring ropes should be less than 15% of the MBL (minimum break load). For a storm condition, the maximum solicitation of a mooring line should not exceed 30% of MBL. Since the loads levels are not high in operation, it may be possible to adapt the proposed theory for yarns to ropes with complex geometric arrangements. In

Table 4
Model parameters (HMPE at room temperature).

$\rho_l E_l$ (N)	R (s)	(S_l/ρ_l) (N^{-1})	K (s^{-1})	(N_l/ρ_l) (N^{-1})	(a_l/ρ_l) (N^{-1})	b
165	10.314	8.47×10^{-4}	4.5×10^{-7}	1.76×10^{-2}	8.36×10^{-4}	0.26

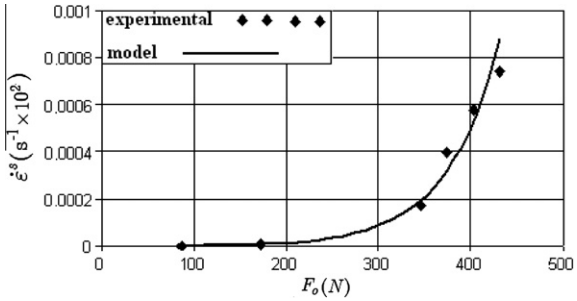

Fig. 9. Secondary creep rate for different load levels. Comparison with experimental results.

Table 5
Secondary creep rate for different load levels.

F_o (N)	$\dot{\varepsilon}^s$ (s^{-1}) experimental	$\dot{\varepsilon}^s$ (s^{-1}) model
86.3	14×10^{-9}	16×10^{-9}
172.6	94×10^{-8}	89×10^{-8}
345.3	17×10^{-7}	19×10^{-7}
374.0	39×10^{-7}	32×10^{-7}
402.7	58×10^{-7}	53×10^{-7}
431.5	74×10^{-7}	88×10^{-7}

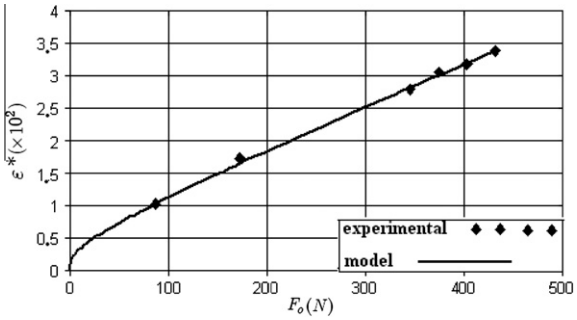

Fig. 10. ε^* for different load levels. Comparison with experimental results.

Table 6
ε^* for different load levels.

F_o (N)	ε^* experimental	ε^* model
86.3	1.02×10^{-2}	1.02×10^{-2}
172.6	1.73×10^{-2}	1.64×10^{-2}
345.3	2.79×10^{-2}	2.80×10^{-2}
374.0	3.05×10^{-2}	3.0×10^{-2}
402.7	3.18×10^{-2}	3.18×10^{-2}
431.5	3.37×10^{-2}	3.38×10^{-2}

Table 7
Creep lifetimes for different load levels.

F_o (N)	t_r (s) experimental	t_r (s) model
345.3	28,710	28,346
374.0	12,162	12,441
402.7	5425	5803
431.5	2935	2846

this case, parameters that appear in the theory would be geometry dependent to account for different possible sub-ropes arrangements. Heating and internal abrasion certainly reduce lifetime but can be accounted in a thermodynamic framework. However, it is important to remark that further experimental work with complex HMPE ropes is required in order to fully characterize the dependency of the parameters on the geometry.

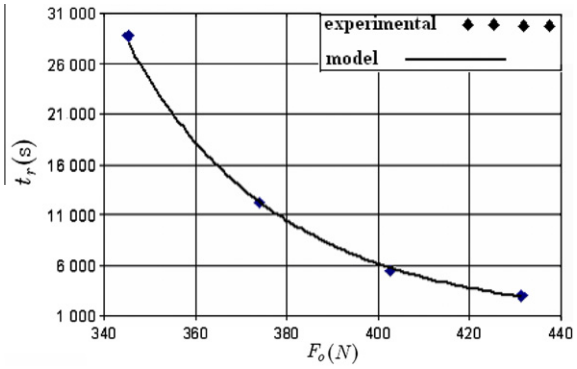

Fig. 11. Creep lifetimes for different load levels. Comparison with experimental results.

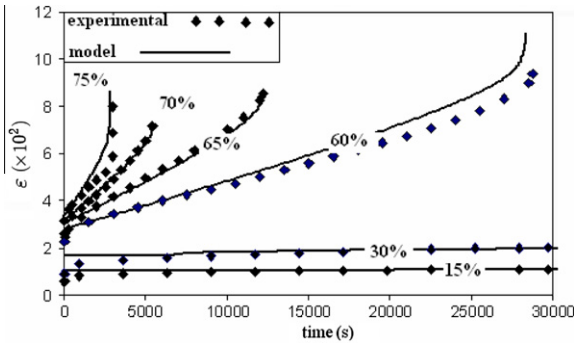

Fig. 12. Creep curves at different load levels. Comparison with experimental results.

Appendix A. Summary of the thermodynamic framework

This Appendix presents the summary of the thermodynamic framework in which the model equations proposed in Section 3.2 can be derived.

When an HMPE specimen of initial gauge length L_o and average fibre area A_o is submitted to a creep test with constant tensile load F_o it may present a complex nonlinear behaviour, mainly after the beginning of the creep damage process, when eventually some of the fibres can break. The main idea of the model is to describe the complex nonlinear behaviour of this system (HMPE yarn) through a one-dimensional and homogeneous "equivalent" continuum model, adequate for processes that can be assumed as quasi-static and isothermal.

A.1. Preliminary definitions

The following version of the FLT holds for a system undergoing quasi-static isothermal processes:

$$\text{FLT} \Rightarrow P_{EXT} = \dot{\Psi} + P_{diss} \tag{A.1}$$

where P_{EXT} is the power of the external forces, Ψ the free energy and P_{diss} the rate of energy dissipation. The FLT Eq. (A.1) can be particularized to the case of a yarn in a creep test in which $P_{EXT} = F_o\dot{\delta}$:

$$\text{FLT} \Rightarrow F_o\dot{\delta} = \dot{\Psi} + P_{diss} \tag{A.2}$$

From Eq. (A.2) it is easy to conclude that, if the free energy Ψ and the dissipated power P_{diss} of both systems (real yard and equivalent spring) are the same at each time instant, then the elongation

rate $\dot{\delta}(t)$ will be the same for both systems $\forall t$. Consequently, the elongation history $\delta(t)$ of both systems will be the same (considering the same initial conditions). Therefore it is necessary to postulate adequate expressions for the free energy Ψ and the dissipated power P_{diss} of the spring in order to obtain an equivalent system (for any tensile load F_o, the elongation history of both systems should be the same). It is interesting to remark that the second law of thermodynamics only requires that:

$$P_{DISS} \geqslant 0 \text{ in all admissible processes} \tag{A.3}$$

A.2. Thermodynamically admissible constitutive equations

The free energy Ψ for the "equivalent" model is supposed to be a differentiable function with the following form:

$$\Psi(\delta,\delta_v,D) = (1-D)\widehat{\Psi}(\delta,\delta_v) = (1-D)\frac{\kappa_o}{2}(\delta-\delta_v)^2 = (1-D)\left(\frac{EA_o}{2L_o}\right)(\delta-\delta_v)^2 \tag{A.4}$$

with δ_v being the irreversible parcel of δ. $\delta_e = \delta - \delta_v$ is the elastic or reversible part of δ. $\kappa_o = (EA_o/L_o)$ is the initial stiffness of the system and E is the modulus of elasticity, a positive material parameters that can be easily identified experimentally.

The main idea adopted in the present work is to introduce an auxiliary damage variable $D \in [0,1]$, associated to the dissipative mechanism of rupture. D is nothing else than an auxiliary variable that accounts for the decrease of the free energy of the system due to the dissipative mechanism of fracture. The system is considered "virgin" if $D = 0$ and it is supposed to no longer resist to the mechanical loading if $D = 1$. Similar expressions can be found in works concerned with elasto-viscoplasticity (see Lemaitre and Chaboche, 1990, for instance).

To complete the theory, additional information must be given in order to characterize the dissipative behaviour. This is done by assuming that:

$$\text{HIP}_2: \text{ if } \dot{D} = \dot{\delta}_v = 0 \Rightarrow P_{DISS} = 0, \quad \forall \dot{\delta} \tag{A.5}$$

HIP_2 states that, since D and δ_v are (global) internal variables related to dissipative mechanisms (damage and viscosity), there is no internal dissipation ($P_{DISS} = 0$) at a given instant t if the material time derivatives of these variables are both equal to zero.

Using the energy Eq. (A.2) and expression (A.4) for the internal energy, the following version of the energy equation can be obtained:

$$\left[F_o - (1-D)\frac{EA_o}{L_o}(\delta-\delta_v)\right]\dot{\delta} + \left[(1-D)\frac{EA_o}{L_o}(\delta-\delta_v)\right]\dot{\delta}_v + \Psi\dot{D} = P_{DISS} \tag{A.6}$$

Since HIP_2 must hold in all processes, from Eqs. (A.5) and (A.6) it is possible to conclude that:

$$F_o = (1-D)\kappa_o(\delta-\delta_v) \Rightarrow \frac{F_o}{A_o} = (1-D)E\left(\frac{\delta}{L_o} - \frac{\delta_v}{L_o}\right) \tag{A.7}$$

and, hence, from (A.6) and (A.7) it results the following version of the energy equation for the spring system:

$$P_{DISS} = [F_o\dot{\delta}_v + \Psi\dot{D}] \tag{A.8}$$

In order to fully characterize the dissipative behaviour, evolution laws must be provided for the internal variables δ_v and D. These evolution laws must be such that they satisfy version (A.3) of the second law of thermodynamics in all processes. Using Eq. (A.8) it comes that, in this particular case, the SLT requires that:

$$P_{DISS} = [F_o\dot{\delta}_v + \Psi\dot{D}] \geqslant 0, \quad \forall(\dot{\delta}_v,\dot{D}) \tag{A.9}$$

The following evolution laws are proposed for the equivalent model:

$$\text{HIP}_3: \ \dot{\delta}_v = \frac{KL_o}{(1-D)}\left[\exp\left(N\frac{F_o}{A_o}\right) - 1\right]; \quad \dot{D} = \left(\frac{2ES^2}{A_oL_o}\widehat{\Psi}(\delta,\delta_v)\right)^{(R/2)} \tag{A.10}$$

where K, N, R and S are positive material constants.

From the evolution laws (A.10) it can be verified that $\dot{\delta}_v \geqslant 0$ and $\dot{D} \geqslant 0$ in all processes. Hence, since $F_o \geqslant 0$ and $\widehat{\Psi} \geqslant 0$, it is possible to conclude that evolution laws (A10) assure that the second law restriction (A.9) is automatically verified in all processes.

Using (A.7) it is possible to verify that $\widehat{\Psi}(\delta,\delta_v) = \frac{L_o}{2EA_o}\left(\frac{F_o}{(1-D)}\right)^2$. Hence, the evolution law for the damage variable D may be expressed in the following alternative form:

$$\dot{D} = \left(\frac{SF_o}{A_o(1-D)}\right)^R \tag{A.11}$$

The so-called state law (A.7) and the evolution laws (A.10) form a complete set of thermodynamically admissible constitutive equations. From these equations, the variable $D(t)$ has a precise definition and can be obtained experimentally.

Eq. (A.7) shows that the damage variable at a given instant t can be obtained experimentally in a creep test with a prescribed force F_o. The specimen is unloaded and the instantaneous elastic recovery corresponds to the elastic or reversible part δ_e of δ. Thus, the global damage variable D at instant t can be evaluated using expression (A7):

$$F_o = (1-D(t))K_o\delta_e(t) \Rightarrow D(t) = 1 - \frac{F_o}{K_o\delta_e(t)} \tag{A.12}$$

Finally, the constitutive equations proposed in Section 3.2 can be obtained defining the global variables $\varepsilon(t)$, $\varepsilon_v(t)$ as follows:

$$\varepsilon(t) = \delta(t)/L_o; \quad \varepsilon_v(t) = \delta_v(t)/L_o$$

Since $A_o = \frac{\rho_l}{\rho}$, from Eqs. (A.7), (A.10) and (A.11) the constitutive equations can be expressed as:

$$\frac{F_o}{A_o} = \frac{\rho F_o}{\rho_l} = (1-D)E(\varepsilon-\varepsilon_v) \Rightarrow F_o = (1-D)\rho_lE_l(\varepsilon-\varepsilon_v) \tag{A.13}$$

$$\dot{\varepsilon}_v = \frac{K}{(1-D)}\left[\exp\left(N\frac{F_o}{A_o}\right) - 1\right] = \frac{K}{(1-D)}\left[\exp\left(N_l\frac{F_o}{\rho_l}\right) - 1\right] \tag{A.14}$$

$$\dot{D} = \left(\frac{SF_o}{A_o(1-D)}\right)^R = \left(\frac{S_lF_o}{\rho_l(1-D)}\right)^R \tag{A.15}$$

where $E_l = E/\rho$, $N_l = \rho N$, $S_l = \rho S$.

References

Beltran, J.F., Williamson, E.B., 2005. Degradation of rope properties under increasing monotonic load. Ocean Engineering 32, 826–844.

Bles, G., Nowacki, W.K., Tourabi, A., 2009. Experimental study of the cyclic visco-elasto-plastic behaviour of a polyamide fibre strap. International Journal of Solids and Structures 46, 2693–2705.

Bonner, M., Duckett, R.A., Ward, I.M., 1999. The creep behaviour of isotropic polyethylene. Journal of Materials Science 34, 1885–1897.

Boxman, R.L.M., Cloos, P.J., 1998. Mooring with synthetic fibers possible in all water depths. Offshore 58 (10), 98.

Costa-Mattos, H.S., Bastos, N., Gomes, J.A.P., 2008. A simple model for slow strain rate and constant load corrosion tests of austenitic stainless steel in acid aqueous solution containing sodium chloride. Corrosion Science 50, 2858–2866.

Chimisso, F.E.G., 2009. Some experimental results regarding creep behavior on synthetic materials used to produce offshore mooring ropes. In: Costa Mattos, H.S., Alves, M. (Eds.), Solid Mechanics in Brazil 2009. ABCM, pp. 69–80.

Ciferri, A., Ward, I.M., 1979. Ultra-high Modulus Polymers. Applied Science, London.

Fernandes, A.C., Rossi, R.R., 2005. Distorted polyester lines for model testing of offshore moored platforms. Ocean Engineering 32, 817–825.

Ghoreishi, S.R., Cartraud, P., Davies, P., Messager, T., 2007. Analytical modeling of synthetic fiber ropes subjected to axial loads – Part I: A new continuum model for multilayered fibrous structures. International Journal of Solids and Structures 44, 2924–2942.

Hooker, J.G., 2000. Synthetic fibre ropes for ultradeep water moorings. In: Drilling and Production Applications, Technical Paper Marlow Ropes, OMT Singapore.

King, M.J., Jearanaisilawong, P., Socrate, S., 2005. A continuum constitutive model for the mechanical behavior of woven fabrics. International Journal of Solids and Structures 42, 3867–3896.

Kolarik, J., Pegoretti, A., Fambri, L., Penati, A., 2006. High-density Polyethylene/cycloolefin copolymer blends, Part 2: Nonlinear tensile creep. Polymer Engineering and Science 46 (10), 1363–1373.

Lemaitre, J., Chaboche, J.L., 1990. Mechanics of Solid Materials. Cambridge University Press.

Liu, H., Polak, M.A., Penlidis, A., 2008. A practical approach to modeling time-dependent nonlinear creep behavior of polyethylene for structural applications. Polymer Engineering and Science 48 (1), 159–167.

Pearson, N.J., 2002. Experimental snap loading of synthetic fiber ropes. Doctoral Thesis, Virginia Polytechnic Institute and State University, Blacksburg.

Pellegrin, I., 1999. Manmade fiber ropes in deepwater mooring applications. In: Offshore Technology Conference, Houston, OTC 10907, 1999, pp. 1–9.

Petruska, D., Geyer, J., Macon, R., Craig, M., Ran, A., Schulz, N., 2005. Polyester mooring for the Mad Dog spar—design issues and other considerations. Ocean Engineering 32 (7), 767–782.

Sampaio, E.M., Bastian, F.L., da Costa-Mattos, H.S., 2004. A simple continuum damage model for adhesively bonded butt joints. Mechanics Research Communications 31 (4), 443–449.

Schmidt, T.M., Bianchini, C., Forte, M.M.C., Amico, S.C., Voronoff, A., Gonçalves, R.C.F., 2006. Socketing of polyester fibre ropes with epoxy resins for deep-water mooring applications. Polymer Testing 25, 1044–1051.

Silva, M.O., Chimisso, F.G.E., 2005. Experimental creep analysis on HMPE synthetic fiber ropes for offshore mooring systems. In: Proceedings of the 18th International Congress of Mechanical Engineering, Ouro Preto, Brazil

Sloan, F., 1999. Synthetics: the future for offshore platform moorings. Sea Technology 40 (4), 49–53.

Smeets, P., Jacobs, M., Mertens, M., 2001. Creep as a design tool for HMPE ropes in long term marine and offshore applications. In: OCEANS, 2001. MTS/IEEE Conference and Exhibition, vol. 2, pp. 685–690.

Ward, I.M., Sweeney, J., 2004. An Introduction to the Mechanical Properties of Solid Polymers, second ed. Wiley.

Wilding, M.A., Ward, I.M., 1981. Creep and recovery in ultrahigh modulus linear polyethylenes. Polymer 22, 870–876.

Wilding, M.A., Ward, I.M., 1984a. Creep and stress-relaxation in ultrahigh modulus linear polyethylene. Journal of Materials Science 19, 629–636.

Wilding, M.A., Ward, I.M., 1984b. Creep-behavior of ultrahigh-modulus polyethylene – influence of draw ratio and polymer composition. Journal of Polymer Science Part B – Polymer Physics 22, 561–575.